Measurement of differential Neutral and Charged Current Cross Sections at High Q^2 from H1

B. Heinemann
DESY, Notkestrasse 85, Hamburg,
22607, Germany
E-mail: bheine@mail.desy.de

Neutral and charged current e^+p cross section measurements at high Q^2 at HERA are presented. The double and single differential neutral and charged current cross sections have been measured in the kinematic range $200 \leq Q^2 \leq 30000$ GeV^2 and $0.005 < x < 0.65$. Parton evolution is tested over four orders of magnitude in Q^2 at high parton momentum fraction x and both measurements are compared to the expectation from the electroweak Standard Model and are found to be in good agreement. At very high $Q^2 > 15000$ GeV^2 and $x \approx 0.45$ a small excess over the expectation is observed with a small statistical significance.

1 Introduction

In Deep Inelastic Scattering at high Q^2 the proton is probed at very short distances $< 10^{-16}$ cm. The incoming positron interacts with a quark in the proton via the exchange of a virtual gauge boson.

The kinematics of this process is given by the center of mass energy $\sqrt{s}$, the virtuality of the gauge boson Q^2, the Bjorken x variable and the inelasticity y. With beam energies of 27.6 and 820 GeV for positrons and protons respectively the center of mass energy at HERA is fixed at $\sqrt{s} \approx 300$ GeV, therefore the process is fully determined by two independent variables x and Q^2.

Based on the luminosity of the 94-96 data taking period an excess of neutral current events compared to the Standard Model expectation has been observed by the H1 [3] and ZEUS [4] collaborations at high values of Q^2 and x. The significance of this excess is tested with a higher luminosity by comparing the neutral and charged current cross section measurements with the expectation given by the electroweak Standard Model and DGLAP evolution.

In neutral current interactions a neutral gauge boson is exchanged, in the Standard Model this is the γ- or Z^0- boson. The leading order Born Cross Section is given in in terms of two structure functions

$$\frac{d^2\sigma^{e^+p\to e^+X}}{dx\, dQ^2} = \frac{2\pi\alpha^2}{xQ^4}\left[Y_+ F_2(x,Q^2) - Y_- xF_3(x,Q^2)\right]$$

where α is the fine structure constant and $Y_\pm = 1 \pm (1-y)^2$. F_2 is the generalized structure function and xF_3 the structure function which contributes due to the γZ interference. They contain the appropriate propagator terms. Therefore, for $Q^2 < 1500$ GeV^2 the influence of xF_3 is very small ($< 2\%$) and increases with Q^2 at high y. In higher order QCD there is an additional longitudinal structure function F_L contributing at high y, the influence is $< 5\%$ at the highest y values and negligible for $y < 0.4$. This measurement is presented in the form of a reduced neutral current cross section defined as

$$\sigma^{NC} \equiv \frac{xQ^4}{2\pi\alpha^2}\frac{1}{Y_+}\frac{\mathrm{d}^2\sigma}{\mathrm{d}x\mathrm{d}Q^2}$$

which conincides with a measurement of F_2 in the region where xF_3 and F_L can be neglected.

The charged current interaction is mediated by a virtual W boson. The leading order QCD Born cross section is given by

$$\frac{d^2\sigma^{e^+p\to\bar{\nu}X}}{dx\,dQ^2} = \frac{G_F^2}{2\pi x}\left(\frac{M_W^2}{(M_W^2+Q^2)}\right)^2 \left(\bar{u}(x,Q^2)+\bar{c}(x,Q^2)+(1-y)^2(d(x,Q^2)+s(x,Q^2))\right)$$

with the Fermi coupling constant G_F and the mass of the W boson M_W.

The reduced charged current cross section is defined in analogy to the neutral current case

$$\sigma^{CC} \equiv \frac{2\pi x}{G_F^2}\frac{(M_W^2+Q^2)^2}{M_W^2}\frac{d^2\sigma}{dx\,dQ^2}$$

2 Experimental Technique

2.1 H1 Detector

The H1 detector is described in detail elsewhere [1]. The most important parts of the H1 detector for the selection of NC and CC events are the Liquid-Argon calorimeter and the central tracking chamber. The Liquid-Argon calorimeter is a sampling calorimeter and consists of an inner electromagnetic and a outer hadronic section. The calorimeter has an angular acceptance of $4^o < \theta < 156^o$ where θ is the polar angle with respect to the proton beam direction. A new *in situ* calibration has been performed in order to reduce the systematic errors on the presented measurements. After this calibration the uncertainty on the electromagnetic energy scale is 1% in the backward region ($\theta_e > 90^o$) and 3% in the forward region. The hadronic energy scale has a uncertainty of 3% (4%) in the forward (backward) part, respectively.

2.2 Kinematic Reconstruction

In neutral current events the kinematic variables can be reconstructed in different ways using observables from the hadronic final state and from the scattered positron. These observables are the energy E'_e and polar angle θ_e of the scattered positron, the quantity $\Sigma = \sum(E_h - p_{z,h})$ and the transverse momentum $P_t = \sqrt{(\sum(p_x,h))^2 + (\sum(p_{y,h})^2)^2}$ of the hadronic final state. For the measurements presented three basic methods have been used:

- electron method:
  $y_e = 1 - \frac{E'_e}{E_e}\sin^2\theta_e/2,$ $\quad Q^2_e = 4E_eE'_e\cos^2\theta_e/2$
- Σ method [5]:
  $y_\Sigma = \frac{\Sigma}{\Sigma+E_e(1-\cos\theta_e)}$, $\quad Q^2_\Sigma = \frac{E_e^2\sin^2\theta_e}{1-y_\Sigma}$
- Jacquet-Blondel method:
  $y_{JB} = \frac{\Sigma}{2E_e},$ $\quad Q^2_{JB} = \frac{P_t^2}{1-y_{JB}}.$

x can be reconstructed for every method from the above variables: $x = \frac{Q^2}{ys}$. The choice of the reconstruction method determines the acceptance, the systematic errors and the radiative corrections. For the neutral current cross section measurement the $e\Sigma$ method was used which uses x from the Σ method ($x_{e\Sigma} \equiv x_\Sigma$) and Q^2 from the electron method ($Q^2_{e\Sigma} \equiv Q^2_e$). It gives a very good resolution in the full kinematic region of the measurement[6]. For the CC cross section measurement the only available method is the Jacquet-Blondel method which has a worse resolution than the methods based on the electron.

2.3 Event Selection

The presented analyses are based on the full luminosity of HERA colliding positrons and protons. The data were taken in 1994-97 and the integrated luminosity amounts to 37 pb^{-1}.

The selection of high Q^2 neutral current events is based on the identification of an electron with high transverse momentum. It is selected by requiring a compact isolated electromagnetic energy deposit in the LAr calorimeter with an energy $E'_e > 11$ GeV, associated to within 12 cm with a track which points to the vertex. Further selection criteria are applied to suppress photoproduction background and to reduce radiative corrections: $y_e < 0.9$ and $\Sigma + E_e(1-\cos\theta_e) > 35$ GeV. The total data sample consists of ca. 75,000 events with a background contamination of $< 5\%$ in any bin.

The main selection criterion for charged current events is a imbalance in transverse momentum, $P_t > 12$ GeV, measured in the Liquid-Argon calorimeter due to the outgoing neutrino which is not detected. In addition for the rejection of photoproduction background the transverse energy flow is required to be predominantly oriented into on hemisphere. Cosmic ray and beam halo background is suppressed by a set of topological background filters and its contamination to the final data sample is about 10 %. The data sample is cleaned from the remaining non-collision background by a visual scan. The total contamination of photoproduction events in the final data sample which consists of about 650 events is less than 1%. The measurement is limited to the range $0.03 < y < 0.9$.

3 Results

The preliminary reduced neutral current cross section measurement by H1 is shown in Fig. 1.a) together with the fixed target BCDMS [10], NMC [9] and SLAC [11] data for $x \geq 0.07$. The result is compared to a NLO DGLAP QCD fit which has been performed to BCDMS, NMC, H1 94 [2] , preliminary low Q^2 95-96 data [12] and the preliminary high Q^2 data presented here. The fit is explained in more detail in [13]. Also shown is the expectation from the MRSH [7] parametrization derived from the very first HERA data [8].

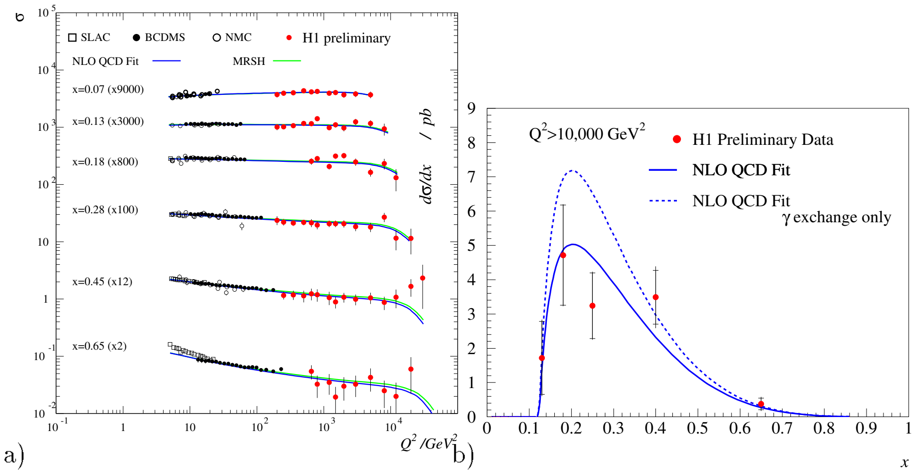

Figure 1: a) The reduced neutral current cross section at high x compared with Standard Model predictions from MRSH and the H1 NLO QCD fit. b) The cross neutral current cross section $d\sigma/dx$ at high Q^2 compared with to expectation from the electroweak Standard Model and to the expectation without the coupling to the Z boson.

The theoretical expectations are shown up to the kinematic limit of HERA. Combining the data of all experiments the cross section has been measured over 4 orders of magnitude in Q^2 in the valence quark region at high $x > 0.1$. At these high x values the data are in good agreement with the QCD predictions up to $Q^2 = 12000$ GeV^2. At the highest Q^2 values the theoretical prediction for the cross section drops due to the influence of the γZ interference term. At $x = 0.45$ the data lie above the expectation [3]. Kinematically this x value can be translated to a mass $M = \sqrt{xs} \approx 200$ GeV.

The neutral current cross section measurement at high Q^2 eventually has a sensitivity to electroweak parameters. This can be seen in Fig. 1 b) where the single differential cross section $d\sigma/dx$ is shown for $Q^2 > 10000$ GeV^2. Also displayed are two theoretical predictions, one corresponding to the Standard Model ($\gamma + Z$ exchange) and one where the Z contribution has been omitted artificially. At low x the two theoretical curves are significantly different and the data favour the Standard Model prediction in prefering the inclusion of a contribution from Z^0 exchange.

Due to higher statistics and improvements in experimental techniques, for the first time, a double differential charged current cross section has been measured for $400 \leq Q^2 \leq 16000$ GeV^2 and $0.015 \leq x \leq 0.5$ at HERA. In Fig. 2.a) it is compared to the Standard Model expectation (MRSH).

The measurement covers the kinematic region where the cross section is dominated by the antiquark density $(\bar{u} + \bar{c})$ in the proton $(x < 0.1)$ as well as the high x region where the dominant contribution arises from the quark density $(d + s)$. In the case of e^+p scattering for $x > 0.2$ the cross section is almost entirely determined by the d valence density. The measurement is in good agreement with the expectation at low and high x in the whole Q^2 range.

The single differential cross section $d\sigma/dQ^2$ is shown for charged current and neutral current scattering in Fig. 2.b) in the kinematic region where both measurements cover the same phase space ($y < 0.9$, $Q^2 > 1000$ GeV^2). It can be seen that the charged current cross section is suppressed by the propagator at low Q^2. With increasing Q^2 the two cross sections approach each other, the remaining difference is due to different helicity dependence and the couplings to different quark flavours in the two processes.

4 Summary

New measurements of neutral and charged current double and single differential cross section have been presented. The focus of these measurements is the kinematic region of high x and high Q^2. It was shown that a fit based on the DGLAP evolution equations is able to describe the double differential neutral

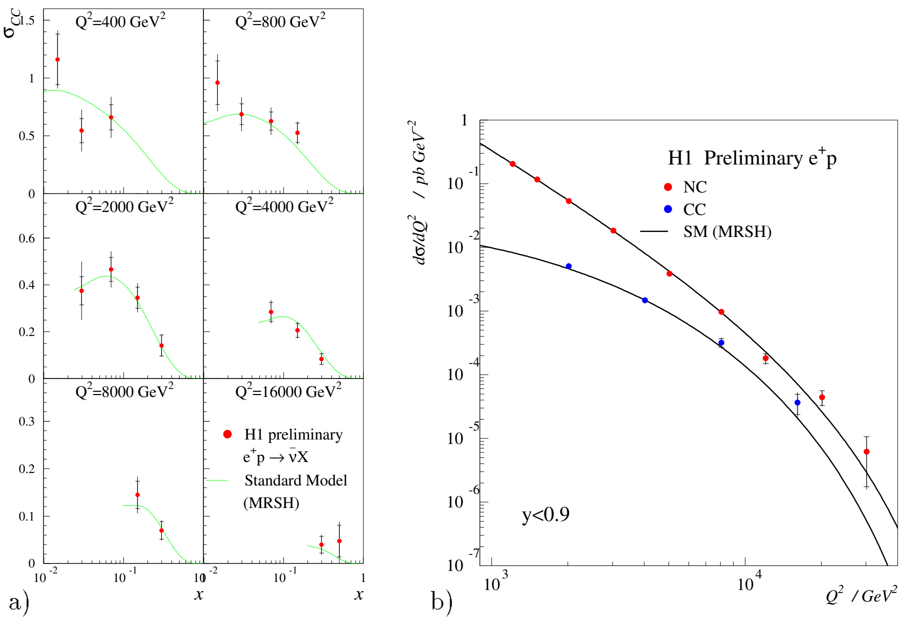

Figure 2: a) The reduced charged current cross section compared with Standard Model predictions from MRSH. b) The charged and neutral current cross section $d\sigma/dQ^2$ at high Q^2 compared with the expectations from the electroweak Standard Model.

current cross section over four orders of magnitude in Q^2 at high x. Both measurements are also in good agreement with the electroweak Standard Model. An excess at high Q^2 remains speculative until sufficiently more integrated luminosity becomes available.

References

1. H1 collaboration, I. Abt et al., Nucl. Instr. and Meth. A386 (1997) 310 and 348
2. H1 collaboration, S. Aid et al., Nucl. Phys. B470(1996) 3.
3. H1 collaboration, C. Adloff et al., Z. Phys. C74 (1997) 191.
4. ZEUS collaboration, J. Breitweg et al., Z. Phys. C74 (1997) 207.
5. U. Bassler, G. Bernardi, Nucl. Instr. and Meth. A361 (1995) 197.
6. U. Bassler, G. Bernardi, DESY-97-137 (1997) 21pp., Submitted to Nucl.Instr. and Meth.
7. A.D. Martin, W.J. Stirling and R.G. Roberts, Phys. Lett. B306 (1993) 145; B309 (1993).

8. H1 collaboration, I. Abt et al., Nucl. Phys. B407 (1993) 515
ZEUS collaboration: M. Derrick et. al., Phys. Lett. B316 (1993) 412
9. NMC Collaboration, M. Arneodo et al., Phys. Lett. B 364 (1995) 107.
10. BCDMS Collaboration, A.C. Benvenuti et al., Phys. Lett. B 223 (1989) 485; CERN preprint CERN-EP/89-06
11. L.W. Whitlow et al., Phys. Lett. B282 (1992) 475;
L.W. Whitlow, preprint SLAC-357 (1990)
12. H1 Collaboration: Paper 262 presented at International Europhysics Conference on HIgh Energy Physics, HEP97, Jerusalem 1997.
13. E. Rizvi, these proceedings